Molecules and Cells

DNAJB9 Inhibits p53-Dependent Oncogene-Induced Senescence and Induces Cell Transformation

Hyeon Ju Lee[1], Yu-Jin Jung[2], Seungkoo Lee[3], Jong-Il Kim[4,5], and Jeong A. Han[1,*]

[1]Department of Biochemistry and Molecular Biology, Kangwon National University School of Medicine, Chuncheon 24341, Korea, [2]Department of Biological Sciences, Kangwon National University, Chuncheon 24341, Korea, [3]Department of Anatomic Pathology, Kangwon National University School of Medicine, Kangwon National University Hospital, Chuncheon 24289, Korea, [4]Genomic Medicine Institute, Medical Research Center, Seoul National University, Seoul 03080, Korea, [5]Department of Biochemistry and Molecular Biology, Seoul National University College of Medicine, Seoul 03080, Korea
*Correspondence: gshja@kangwon.ac.kr
https://doi.org/10.14348/molcells.2020.2231
www.molcells.org

DNAJB9 **is known to be a member of the molecular chaperone gene family, whose cellular function has not yet been fully characterized. Here, we investigated the cellular function of DNAJB9 under strong mitogenic signals. We found that DNAJB9 inhibits p53-dependent oncogene-induced senescence (OIS) and induces neoplastic transformation under oncogenic RAS activation in mouse primary fibroblasts. In addition, we observed that DNAJB9 interacts physically with p53 under oncogenic RAS activation and that the p53-interacting region of DNAJB9 is critical for the inhibition of p53-dependent OIS and induction of neoplastic transformation by DNAJB9. These results suggest that DNAJB9 induces cell transformation under strong mitogenic signals, which is attributable to the inhibition of p53-dependent OIS by physical interactions with p53. This study might contribute to our understanding of the cellular function of DNAJB9 and the molecular basis of cell transformation.**

Keywords: DNAJB9, p53, RAS, senescence, transformation

INTRODUCTION

During the malignant transformation process, normal cells acquire the capability to sustain growth signaling by oncogenic activation of mitogenic genes (Hanahan and Weinberg, 2000; 2011). However, previous studies showed that cells having the intact DNA damage response (DDR) pathway and high levels of $p16^{INK4A}$ expression undergo senescence in response to strong mitogenic signals caused by several mitogenic oncogenes including $H\text{-}RAS^{V12}$ (Bartkova et al., 2006; Benanti and Galloway, 2004; Courtois-Cox et al., 2008; Di Micco et al., 2007; Sarkisian et al., 2007; Serrano et al., 1997). This phenomenon named as oncogene-induced senescence (OIS) is reported in cultured cells as well as in premalignant tissues from mice and humans (Sarkisian et al., 2007; Serrano et al., 1997). Therefore, OIS is thought to be a barrier to malignant transformation by eliminating premalignant cells via the immune system (Halazonetis et al., 2008; Kang et al., 2011).

p53, the best-known tumor suppressor, plays a key role in the OIS. Sustained growth signals by those mitogenic oncogenes results in the DNA replication stress and DNA double-strand breaks, which triggers the DDR involving p53 ac-

Received 11 October, 2019; revised 25 February, 2020; accepted 26 February, 2020; published online 8 April, 2020

eISSN: 0219-1032

tivation (Bartkova et al., 2005; 2006; Di Micco et al., 2006). Then, as a transcription factor, p53 moves to the nucleus and binds to the promoter of senescence-mediating target genes such as $p21^{WAF1/CIP1}$, resulting in OIS (Campisi and d'Adda di Fagagna, 2007; Nardella et al., 2011). In normal mouse or rat fibroblasts, p53 knockout can overcome OIS and induce malignant transformation (Akagi, 2004; Serrano et al., 1997). In normal human fibroblasts, p53 knockout can or cannot overcome OIS (Bartkova et al., 2006; Campisi and d'Adda di Fagagna, 2007; Di Micco et al., 2006; Narita et al., 2003; Serrano et al., 1997), and malignant transformation additionally requires inactivation of pRb and PP2A as well as activation of telomerase (Akagi, 2004; Zhao et al., 2004).

Chaperone proteins bind their substrate proteins to assist the substrate protein's proper folding, oligomeric assembly, protein trafficking, or degradation. The heat shock protein 70s (HSP70s), the major chaperones in most eukaryotes, have the ATPase domain and interconvert between the ATP-bound low affinity state and the ADP-bound high affinity state for the substrate proteins. DNAJ proteins are co-chaperones that regulate the activity of HSP70s: they bind to HSP70s and promote the ATPase activity, which leads to the conversion of HSP70s from the low affinity state to the high affinity state (Hartl et al., 2011). Human has been reported to have at least 41 DNAJ proteins. They commonly have the J domain, which is an essential region for binding to HSP70s and enhancing the ATPase activity (Qiu et al., 2006).

DNAJB9, a member of the DNAJ protein family, also has the J domain consisting of 70 amino acids (Qiu et al., 2006; Vos et al., 2008). It has been reported that DNAJB9 is an endoplasmic reticulum (ER)-resident protein and has a co-chaperone activity for binding immunoglobulin protein (BiP), the major HSP70 in the ER (Qiu et al., 2006; Shen et al., 2002; Vos et al., 2008). In addition, DNAJB9 has been reported to prevent cell death induced by tunicamycin, an ER stressor, in SK-N-SH cells (Kurisu et al., 2003), but the cellular function of this protein has been largely unknown.

We have previously reported that DNAJB9 inhibits p53-dependent apoptosis under genotoxic conditions (Lee et al., 2015), leading us to hypothesize that DNAJB9 might contribute to cell transformation by regulating the pro-senescent function of p53 under strong mitogenic signals. In this study, we investigate this possibility and provide evidence that DNAJB9 inhibits p53-dependent OIS and induces cell transformation under strong mitogenic signals.

MATERIALS AND METHODS

Cell culture

Mouse embryonic fibroblasts (MEFs) (Jozefczuk et al., 2012), human diploid fibroblasts (HDFs) (Kim et al., 2008), and Saos-2 cells were maintained in Dulbecco's modified Eagle's medium (DMEM) containing 10% fetal bovine serum (#F60001; Median Life Science, USA), penicillin (100 units/ml), and streptomycin (100 units/ml) in a 5% CO_2 incubator.

Retroviruses

cDNAs of human DNAJB9, $H\text{-}RAS^{V12}$, p53, and SV40 LT were cloned into the pMSCVpuro vector (Clontech, USA), and retroviruses were produced in H29D packaging cells as described previously (Ory et al., 1996). Conditioned media containing retroviruses were collected and administered into cells in the presence of 2 μg/ml polybren. Cells were selected in 1 μg/ml puromycin for 2 days and then seeded for various assays.

SA-β-gal staining

Senescence-associated β-galactosidase (SA-β-gal) staining was carried out at pH 6.0 as described previously (Dimri et al., 1995). Briefly, cells were washed with phosphate-buffered saline (PBS), fixed in 3% formaldehyde for 5 min, and then stained at 37°C in a solution containing 1 mg/ml X-gal, 40 mM citric acid/sodium phosphate, pH 6.0, 5 mM potassium ferrocyanide, 5 mM potassium ferricyanide, 150 mM sodium chloride and 2 mM magnesium chloride (Kim et al., 2008). After 24 h, cells were photographed at 100× magnification using an Olympus CKK41SF light microscope (Olympus, Japan). Cells (100-200 cells per sample) were examined and the ratios of stained cells were calculated.

Western blot analysis

Cells were lysed in a lysis buffer (150 mM NaCl, 50 mM Tris–HCl, 1% NP-40, 0.25% sodium deoxycholate, and 0.1% SDS) with 1 mM PMSF, 1 μg/ml aprotinin, 1 μg/ml leupeptin and 1 μg/ml pepstatin. Proteins were resolved on 10% or 12% SDS–polyacrylamide gels and transferred to PVDF membranes, which were probed with specific antibodies. The immunoreactive protein complexes were detected by enhanced chemiluminescence (Amersham Bioscience, UK) (Choi et al., 2009). The specific antibodies used in this study were as follows: an anti-DNAJB9 polyclonal antibody raised against a synthetic peptide (Kurisu et al., 2003; Lee et al., 2015), an anti-Pan-Ras monoclonal antibody (OP40; Calbiochem, USA), an anti-p53 polyclonal antibody (sc-6243; Santa Cruz Biotechnology, USA), an anti-phospho-p53 (Ser15) polyclonal antibody (#9284; Cell Signaling Technology, USA), an anti-$p21^{WAF1/CIP1}$ polyclonal antibody (sc-397; Santa Cruz Biotechnology), and an anti-β-actin monoclonal antibody (sc-81178; Santa Cruz Biotechnology).

Immunoprecipitation

MEFs infected with retroviruses were lysed in a lysis buffer (50 mM Tris-HCl, pH 7.4, 150 mM NaCl, 1% NP-40, 0.25% sodium deoxycholate, 0.1% SDS, 50 mM NaF, 1 mM sodium orthovanadate, and a protease inhibitor cocktail). Cell lysates were precleared and incubated with an anti-DNAJB9 polyclonal antibody raised against a synthetic peptide (Kurisu et al., 2003; Lee et al., 2015) at 4°C overnight, followed by mixing with 20 μl of Protein A/G PLUS-agarose beads (sc-2003; Santa Cruz Biotechnology) for 2 h at 4°C. The beads were collected and washed with the lysis buffer. Then, bead-bound proteins were subjected to western blot analysis using an anti-p53 monoclonal antibody (1c12, #2524; Cell Signaling Biotechnology, USA) and the anti-DNAJB9 polyclonal antibody.

Confocal microscopy

MEFs infected with retroviruses were seeded onto 18 mm

coverslips and cultured overnight. The next day, cells were fixed with 3.7% formaldehyde and permeabilized with 0.2% Triton X-100. After blocking with 2% bovine serum albumin, cells were incubated with an anti-DNAJB9 polyclonal antibody (1:100) and an anti-p53 monoclonal antibody (1c12, #2524, 1:100) at 4°C overnight. Cells were then incubated with a TRITC-conjugated anti-rabbit IgG (A-21428, 1:200; Invitrogen, USA) or a FITC-conjugated anti-mouse IgG (F6257, 1:200; Sigma-Aldrich, USA) for 1 h at room temperature. After the nuclei were stained with 1 μg/ml DAPI (D9542; Sigma-Aldrich) for 10 min, cell images were taken with a confocal microscope (Carl Zeiss, Germany) (Kuk et al., 2019; Lee et al., 2015).

Soft agar assay

MEFs (2.5×10^4 cells) were suspended in culture medium with 0.35% low-melting agarose and seeded on the 0.5% solidified agarose (Sigma-Aldrich). After 4 to 5 weeks, the to-

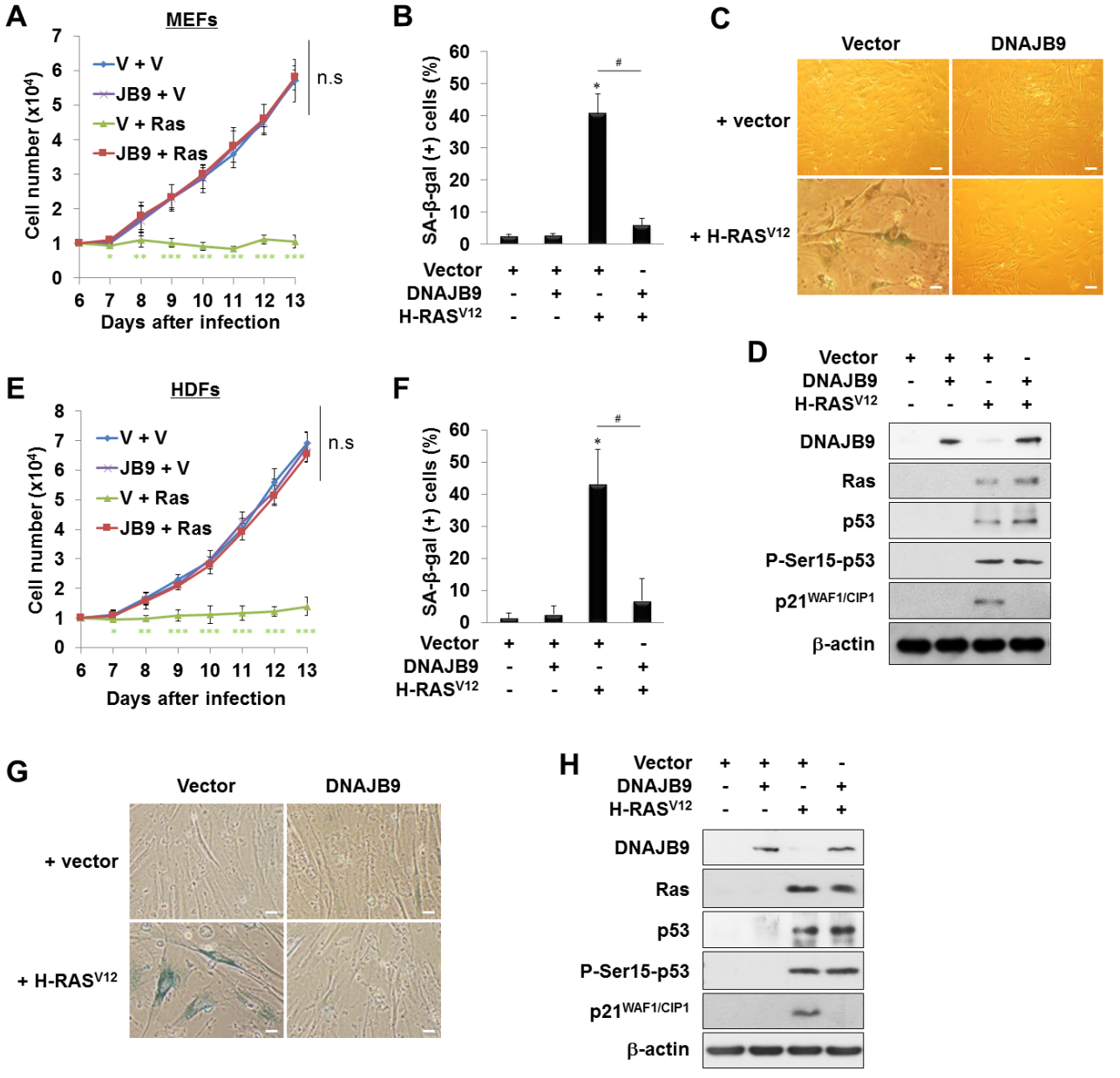

Fig. 1. DNAJB9 inhibits H-RAS^{V12}-induced senescence in MEFs (A-D) and HDFs (E-H). (A and E) Cells were infected with retroviruses as indicated (V, vector; JB9, DNAJB9; Ras, H-RAS^{V12}). Then, 1×10^4 cells were seeded and the number of cells was counted. Data are represent as mean ± SD (n = 6; $*P < 0.05$, $**P < 0.01$, $***P < 0.001$ vs V + V; n.s, not significant). (B and F) The ratios of SA-β-gal (+) cells were calculated. Data are represent as mean ± SD (n = 8; $*P < 0.05$ vs vector, $^{\#}P < 0.05$). (C and G) Representative SA-β-gal staining data were shown. Scale bars = 13.6 μm. (D and H) Western blot analysis was performed with cell lysates. β-Actin was used as a loading control.

tal number of foci per sample was counted using an Olympus CKK41SF light microscope at 100× magnification.

In vivo tumor formation assay

All procedures were approved by the Institutional Animal Care and Use Committee of the Kangwon National University (KW-140521-1) and were conducted in accordance with the Guidelines for the Care and Use of Laboratory Animals. Female BALB/c nude mice were purchased from Nara Biotech (Korea). Four mice per group were injected in each flank with 1×10^6 cells in 100 μl of PBS. Tumor volumes were calculated with the formula $x^2 \times y/2$, where x is the width and y is the length as described (Tomayko and Reynolds, 1989).

Statistical analysis

We performed non-parametric Kruskal–Wallis tests for entire dataset and Wilcoxon rank sum tests for specific two groups of interest by using the RStudio program ver. 1.2.1355 (RStudio, USA; https://www.rstudio.com). Differences between groups were considered statistically significant when the *P* values were < 0.05 (Choi et al., 2009).

RESULTS

DNAJB9 overexpression inhibits oncogene-induced senescence under oncogenic RAS activation

Activation of mitogenic oncogenes such as *H-RAS*^{V12} results in OIS in normal cells (Di Micco et al., 2007; Halazonetis et al., 2008). Therefore, to investigate the cellular function of DNAJB9 under strong mitogenic signals, we first investigated the role of DNAJB9 in OIS induced by H-RAS^{V12}. When we infected MEFs with retroviruses expressing H-RAS^{V12}, it was observed that cell proliferation ceased and the ratios of senescence-associated β-galactosidase (SA-β-gal) (+) cells increased as described (Serrano et al., 1997). In contrast, when we transfected MEFs with both DNAJB9 and H-RAS^{V12}, cells proliferated well and the SA-β-gal (+) cell ratios were reduced to basal levels (Figs. 1A-1C). In addition, expression of senescence-mediating genes such as *p53* and *p21*$^{WAF1/CIP1}$ as well as the phosphorylation of p53 were increased by H-RAS^{V12} transfection as expected (Serrano et al., 1997). Intriguingly, expression of *p21*$^{WAF1/CIP1}$—a known senescence-mediating target gene of p53—decreased in the DNAJB9/H-RAS^{V12}-transfected MEFs compared to the H-RAS^{V12}-transfected MEFs

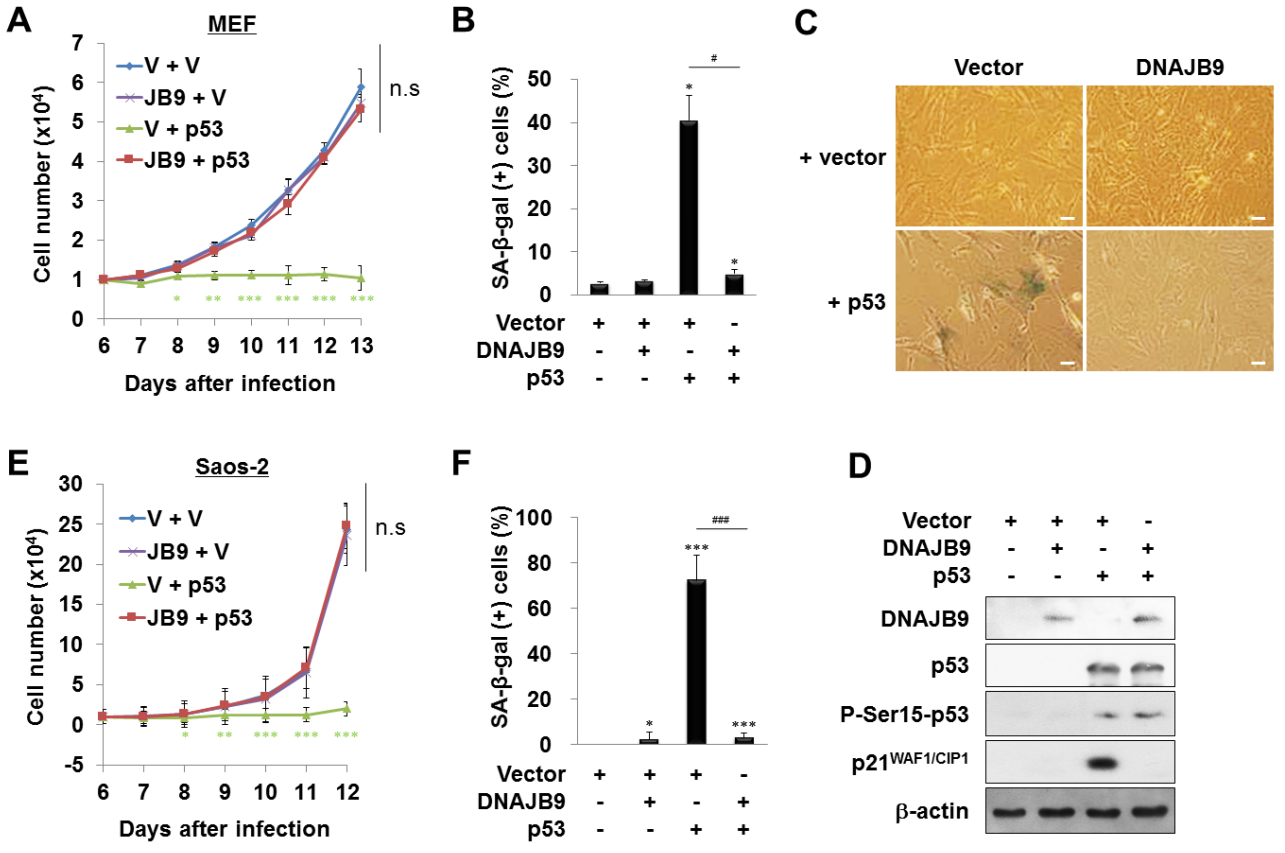

Fig. 2. DNAJB9 inhibits p53-induced senescence in MEFs (A-D) and Saos-2 cells (E and F). (A and E) Cells were infected with retroviruses as indicated (V, vector; JB9, DNAJB9). Then, 1×10^4 cells were seeded and the number of cells was counted. Data are represent as mean ± SD for (A) and SEM for (E) (n = 5; $*P < 0.05$, $**P < 0.01$, $***P < 0.001$ vs V + V; n.s, not significant). (B and F) The ratios of SA-β-gal (+) cells were calculated. Data are represent as means ± SD (n = 6 for Fig. 2B and n = 9 for Fig. 2F; $*P < 0.05$, $***P < 0.001$ vs vector, $^{\#}P < 0.05$, $^{\#\#\#}P < 0.001$). (C) Representative SA-β-gal staining data was shown. Scale bars = 13.6 μm. (D) Western blot analysis was performed with cell lysates. β-Actin was used as a loading control.

without alterations in the level of total and phosphorylated p53 (Fig. 1D). These results suggest that DNAJB9 inhibits OIS under strong mitogenic signals by inhibition of the p53-dependent senescence in normal murine cells.

To examine the role of DNAJB9 under mitogenic oncogene activation in normal human cells, we infected HDFs with retroviruses expressing H-RAS^{V12}. It was observed that cell proliferation ceased and the SA-β-gal (+) cell ratios increased by the H-RAS^{V12} transfection. However, when we transfected HDFs with both DNAJB9 and H-RAS^{V12}, cells proliferated well and the SA-β-gal (+) cell ratios were reduced to basal levels (Figs. 1E-1G). In addition, expression levels of p53 and p21$^{WAF1/CIP1}$ were increased by H-RAS^{V12} transfection. Again, expression levels of p21$^{WAF1/CIP1}$ decreased in the DNAJB9/H-RAS^{V12}-transfected HDFs compared to the H-RAS^{V12}-transfected HDFs (Fig. 1H). These results suggest that DNAJB9 inhibits OIS under strong mitogenic signals by inhibition of the p53-dependent senescence in normal human cells, too.

DNAJB9 overexpression inhibits p53-induced senescence

To confirm the inhibitory effect of DNAJB9 on the p53-dependent senescence, we examined the role of DNAJB9 in the senescence induced by p53 overexpression. When we infected MEFs with retroviruses expressing p53, it was observed that cell proliferation ceased and the ratios of SA-β-gal (+) cells increased as expected (Ferbeyre et al., 2002). In contrast, when we transfected MEFs with both DNAJB9 and p53, cells proliferated well and the ratios of SA-β-gal (+) cells were reduced to basal levels (Figs. 2A-2C). In addition, expression levels of p21$^{WAF1/CIP1}$ were reduced in the DNAJB9/p53-transfected MEFs compared to the p53-transfected MEFs (Fig. 2D). These results suggest that DNAJB9 inhibits p53-induced senescence, supporting our conclusion that DNAJB9 inhibits OIS by inhibition of the p53-dependent senescence.

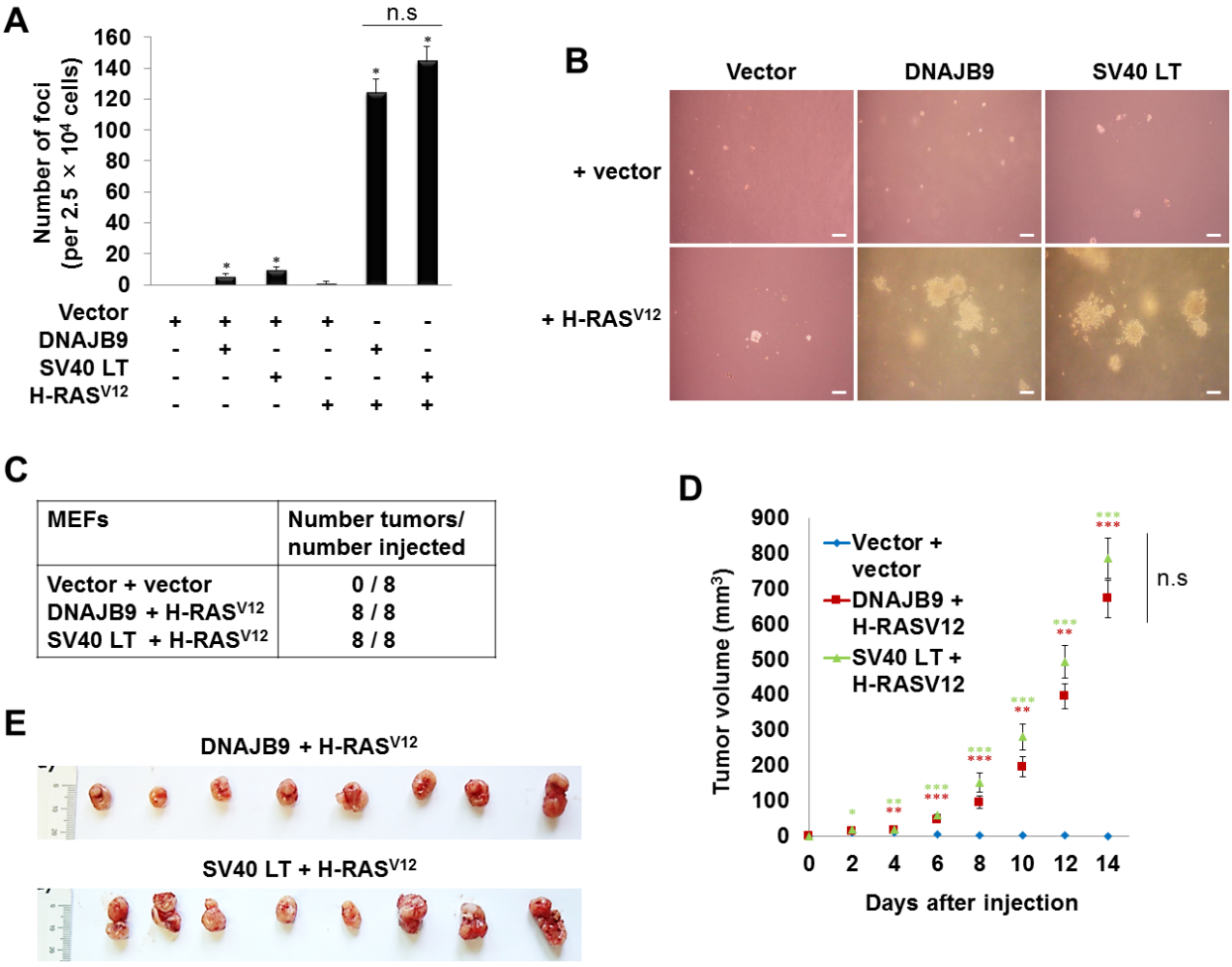

Fig. 3. DNAJB9 induces neoplastic transformation with H-RAS^{V12} in MEFs. (A) Soft agar assay. MEFs were infected with retroviruses as indicated. Then, 2.5 × 10^4 cells were seeded on the soft agar and the total number of foci was counted. Data are represent as mean ± SD (n = 4; $*P < 0.05$ vs vector; n.s, not significant). (B) Representative data of soft agar assay was shown. Scale bars = 100 μm. (C-E) *In vivo* tumor formation assay. MEFs were infected with retroviruses and injected into nude mice. Total number of tumors per group (C), tumor volumes (D), and resected tumors (E) were shown. Data are represent as mean ± SEM (n = 8; $*P < 0.05$, $**P < 0.01$, $***P < 0.001$ vs vector + vector; n.s, not significant).

To further verify the effect of DNAJB9 on p53-induced senescence, we monitored the effect of DNAJB9 overexpression in *p53*-null Saos-2 cells. When we infected retroviruses expressing p53 in Saos-2 cells, cell proliferation ceased and the SA-β-gal (+) cell ratios increased as expected. In contrast, when we transfected Saos-2 cells with both DNAJB9 and p53, cells proliferated well and the SA-β-gal (+) cell ratios were reduced to basal levels (Figs. 2E and 2F). These results confirm that DNAJB9 inhibits p53-induced senescence, again supporting our conclusion that DNAJB9 prevents OIS by inhibition of the p53-dependent senescence.

DNAJB9 overexpression induces neoplastic transformation with H-RAS^{V12} in MEFs

Since overcoming OIS is sufficient to induce malignant transformation in normal rodent cells (Akagi, 2004; Serrano et al., 1997), we then investigated whether DNAJB9 could induce transformation in MEFs.

When we transfected MEFs with H-RAS^{V12}, cells rarely formed foci on the soft agar as expected. In contrast, when we transfected MEFs with both DNAJB9 and H-RAS^{V12}, cells readily formed foci on the soft agar as the simian virus 40 large T (SV40 LT)/H-RAS^{V12}-transfected MEFs, the positive

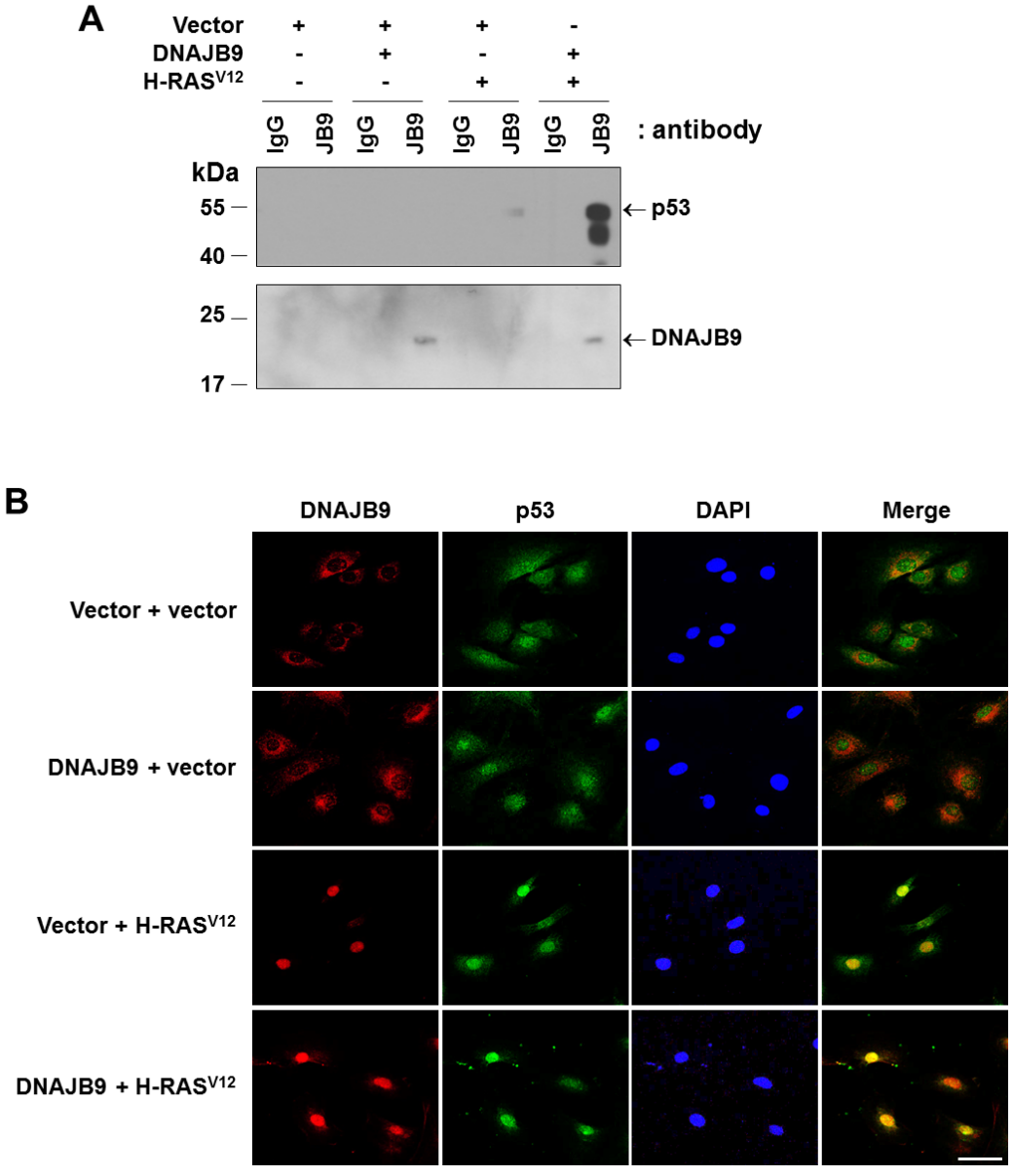

Fig. 4. DNAJB9 interacts physically with p53 under H-RAS^{V12} expression. MEFs were infected with retroviruses as indicated. (A) Cell lysates were subjected to immunoprecipitation using an anti-DNAJB9 antibody, followed by western blotting using an anti-p53 antibody (1c12) (upper panel) and the anti-DNAJB9 antibody (lower panel). (B) Confocal microscopy was performed using an anti-DNAJB9 antibody (red), an anti-p53 antibody (green), and DAPI (blue) as described in Materials and Methods section. Merged images of red and green channels were also shown. Scale bar = 50 μm. Magnification, 400×.

control, did (Figs. 3A and 3B). In addition, the DNAJB9/H-RAS^{V12}-transfected MEFs readily formed tumors in all injected sites of nude mice as the SV40 LT/H-RAS^{V12}-transfected MEFs did (Figs. 3C-3E). These results suggest that DNAJB9 induces cell transformation under strong mitogenic signals.

DNAJB9 overexpression inhibits p53- and H-RAS^{V12}-induced senescence by physical interactions with p53

We next investigated the mechanism by which DNAJB9 inhibits p53- and H-RAS^{V12}-induced senescence. Since DNAJB9 is a molecular chaperone that has the ability to bind other proteins (Hartl et al., 2011) and it has been reported that DNAJB9 interacts physically with p53 through the J domain (Lee et al., 2015), we assumed that DNAJB9 might inhibit the p53- and H-RAS^{V12}-induced senescence through physical interactions with p53.

To test this possibility, we performed an immunoprecipitation assay using an anti-DNAJB9 antibody in MEFs. The data showed that p53 was co-precipitated with DNAJB9 under H-RAS^{V12} transfection and the amount of precipitated p53 was increased dramatically by DNAJB9 overexpression (Fig. 4A). These results suggest that DNAJB9 interacts physically with p53 under strong mitogenic signals and that DNAJB9 overexpression may inhibit p53- and H-RAS^{V12}-induced senescence by physical interactions with p53.

To determine the location of the DNAJB9-p53 interaction, we performed a confocal microscopy in MEFs. In the absence of H-RAS^{V12} transfection, DNAJB9 was observed in the perinuclear region as expected, while p53 was observed in the nucleus and cytoplasm. Upon H-RAS^{V12} transfection, we observed that DNAJB9 translocates to the nucleus while p53 is concentrated in the nucleus, showing that DNAJB9 co-localizes with p53 in the nucleus (Fig. 4B). These results suggest that DNAJB9 interacts physically with p53 in the nucleus under strong mitogenic signals and that DNAJB9 overexpression may inhibit p53- and H-RAS^{V12}-induced senescence by physical interactions with p53 in the nucleus.

To examine whether the DNAJB9-p53 interaction is involved in DNAJB9-mediated inhibition of p53- and H-RAS^{V12}-induced senescence, we produced retroviruses expressing $(myc)_6$-tagged DNAJB9 deletion mutants containing the full-length (FL, amino acids 1-223); the J domain (JD, amino acids 24-93); and a carboxy-terminal region (CT, amino acids 154-223) as a negative control (Fig. 5A). When we infected MEFs with retroviruses expressing the DNAJB9 deletion mutants, it was observed that DNAJB9-FL and -JD prevented the p53-induced growth arrest and SA-β-gal activities, but DNAJB9-CT did not (Figs. 5B-5D). In addition, DNAJB9-FL and -JD prevented the H-RAS^{V12}-induced growth arrest and SA-β-gal activities, but DNAJB9-CT did not (Figs. 5E and 5F). These results demonstrate the critical role of the J domain for DNAJB9 to inhibit p53- and H-RAS^{V12}-induced senescence, suggesting that DNAJB9 inhibits p53- and H-RAS^{V12}-induced senescence by physical interactions with p53.

The DNAJB9-p53 interaction is involved in DNAJB9-mediated neoplastic transformation

Since our data suggest that DNAJB9 inhibits OIS by physical interactions with p53, we finally asked whether the DNAJB9-p53 interaction is involved in the DNAJB9-mediated transformation.

When we transfected MEFs with DNAJB9 deletion mutants with H-RAS^{V12}, it was observed that cells transfected with DNAJB9-FL and -JD formed foci readily on the soft agar, whereas cells transfected with DNAJB9-CT did not (Figs. 6A and 6B). In addition, the DNAJB9-FL and -JD-transfected MEFs formed tumors readily in all injected sites of nude mice (Figs. 6C-6E). These results demonstrate the critical role of the J domain for DNAJB9 to induce neoplastic transformation, suggesting that the physical interaction between DNAJB9 and p53 is involved in the DNAJB9-mediated transformation.

DISCUSSION

DNAJB9 has been known to be a molecular co-chaperone that assists the function of the major chaperone BiP (Awe et al., 2008; Shen et al., 2002). In addition, DNAJB9 has been reported to be a survival factor preventing cell death induced by tunicamycin or DNA damaging agents (Kurisu et al., 2003; Lee et al., 2015). The cellular function of DNAJB9, however, has not been fully understood. We here report a novel function of DNAJB9, an anti-senescent factor and a proto-oncogene candidate, as evidenced by the results that DNAJB9 inhibits the H-RAS^{V12}- and p53-induced senescence (Figs. 1 and 2) and induces cell transformation (Fig. 3). Since DNAJB9 is a molecular co-chaperone whose entity is to bind proteins, there is a possibility that DNAJB9 could bind not only to p53 but also to other senescence-regulating proteins including p16^{INK4A} or Rb, through which it regulates OIS and contributes to cell transformation. Further studies are required to elucidate this possibility.

We here also provided the mechanism for the DNAJB9-mediated inhibition of p53-dependent senescence and induction of cell transformation. DNAJB9 inhibits the p53-dependent senescence by physical interactions with p53 (Figs. 4 and 5B-5D), by which it prevents OIS and induces neoplastic transformation (Figs. 5E, 5F, and 6). According to our data, DNAJB9 overexpression does not down-regulate the level of total p53 or phosphorylated p53 under H-RAS^{V12} or p53 transfection (Figs. 1D, 1H, and 2D). This suggests that the DNAJB9-p53 interaction is not involved in p53 degradation or phosphorylation. Instead, our data show that DNAJB9 co-localizes with p53 in the nucleus under H-RAS^{V12} transfection (Fig. 4B), suggesting that DNAJB9 may inhibit p53 activity through its interaction with p53 in the nucleus. Further studies are required to elucidate the exact function of DNAJB9 in the nucleus. It is worth mentioning that although both H-RAS^{V12} transfection and DNAJB9/H-RAS^{V12} transfection induce nuclear translocation of DNAJB9 (Fig. 4B), H-RAS^{V12} transfection induces cell senescence whereas DNAJB9/H-RAS^{V12} transfection prevents senescence (Fig. 1). As the cause of this phenomenon, we assume that the amount of endogenous DNAJB9 is not sufficient to overcome p53 activity in the nucleus of H-RAS^{V12}-transfected cells, whereas the amount of DNAJB9 is sufficient to overcome p53 activity in the nucleus of DNAJB9/H-RAS^{V12}-transfected cells. In line with this idea, the amount of p53 precipitated by an anti-DNAJB9 antibody is very small

in H-RAS^{V12}-transfected cells, whereas it is dramatically increased in DNAJB9/H-RAS^{V12}-transfected cells (Fig. 4A).

Intriguingly, the p53-interacting region of DNAJB9, the J domain, has a homology among the DNAJ proteins (Qiu et al., 2006; Walsh et al., 2004), suggesting that other DNAJ proteins could also inhibit p53-dependent senescence and contribute to transformation by protein-protein interactions with p53. Of note, it has been reported that DNAJA3 interacts with p53 in the mitochondria through the J domain to promote p53-dependent apoptosis under the treatment of desferroxamine mesylote, an iron chelator, in MCF-7 cells (Ahn et al., 2010; Trinh et al., 2010), suggesting that the J domain effect on p53 might vary depending on the DNAJ protein or on the location of the interaction.

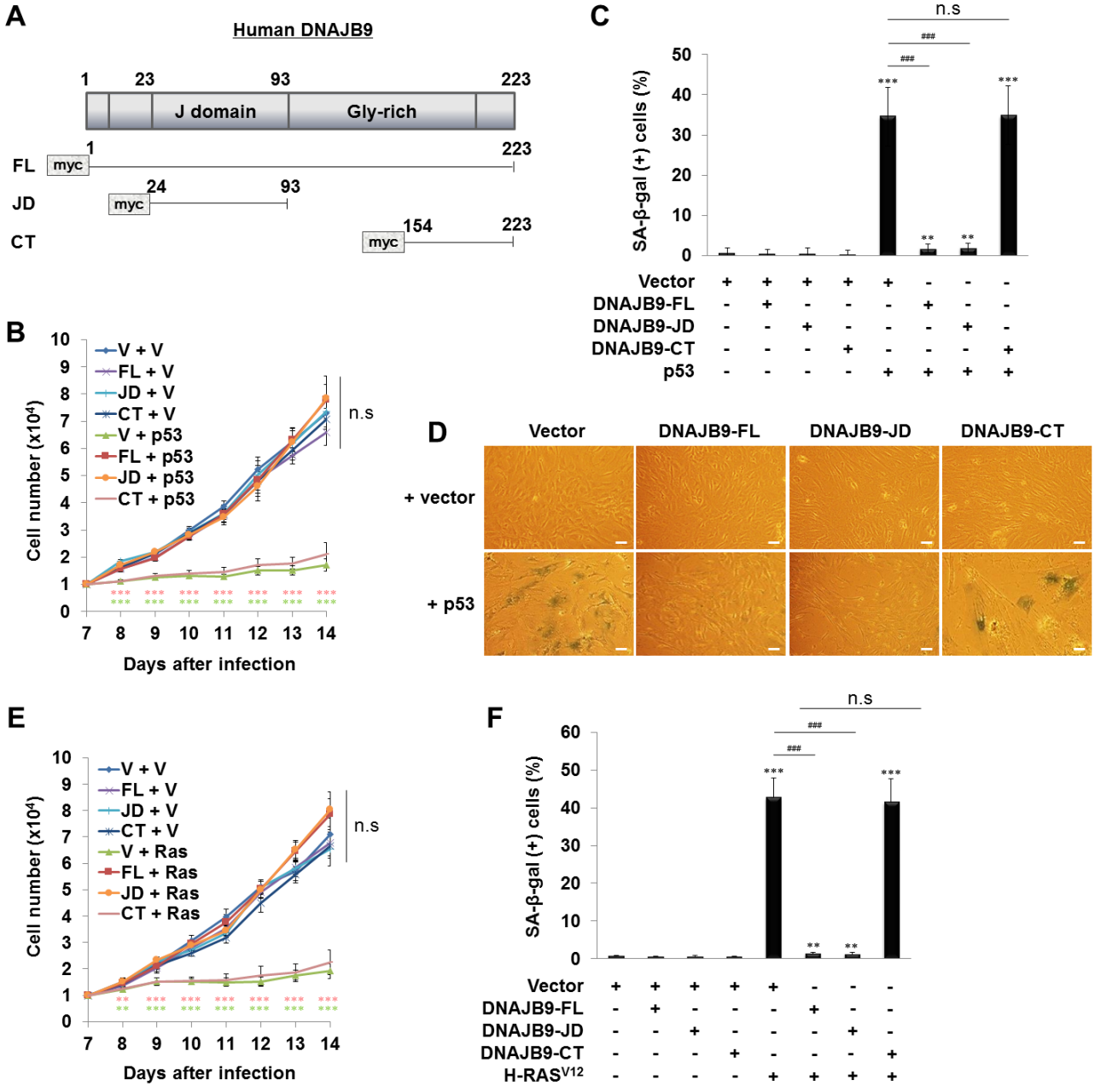

Fig. 5. The DNAJB9-p53 interaction is involved in DNAJB9-mediated inhibition of p53- (B-D) and H-RAS^{V12}-induced senescence (E and F). (A) A schematic representation of the structure of human DNAJB9 and its deletion mutants. (B and E) MEFs were infected with retroviruses as indicated (V, vector; Ras, H-RAS^{V12}). Then, 1 × 10^4 cells were seeded and the number of cells was counted. Data are represent as mean ± SEM (n = 15 for Fig. 5B and n = 10 for Fig. 5E; $^{**}P < 0.01$, $^{***}P < 0.001$ vs V + V; n.s, not significant). (C and F) The ratios of SA-β-gal (+) cells were calculated. Data are represent as mean ± SD (n = 26 for Fig. 5C and n = 8 for Fig. 5F; $^{**}P < 0.01$, $^{***}P < 0.001$ vs vector, $^{###}P < 0.001$; n.s, not significant). (D) Representative SA-β-gal staining data was shown. Scale bars = 13.6 μm.

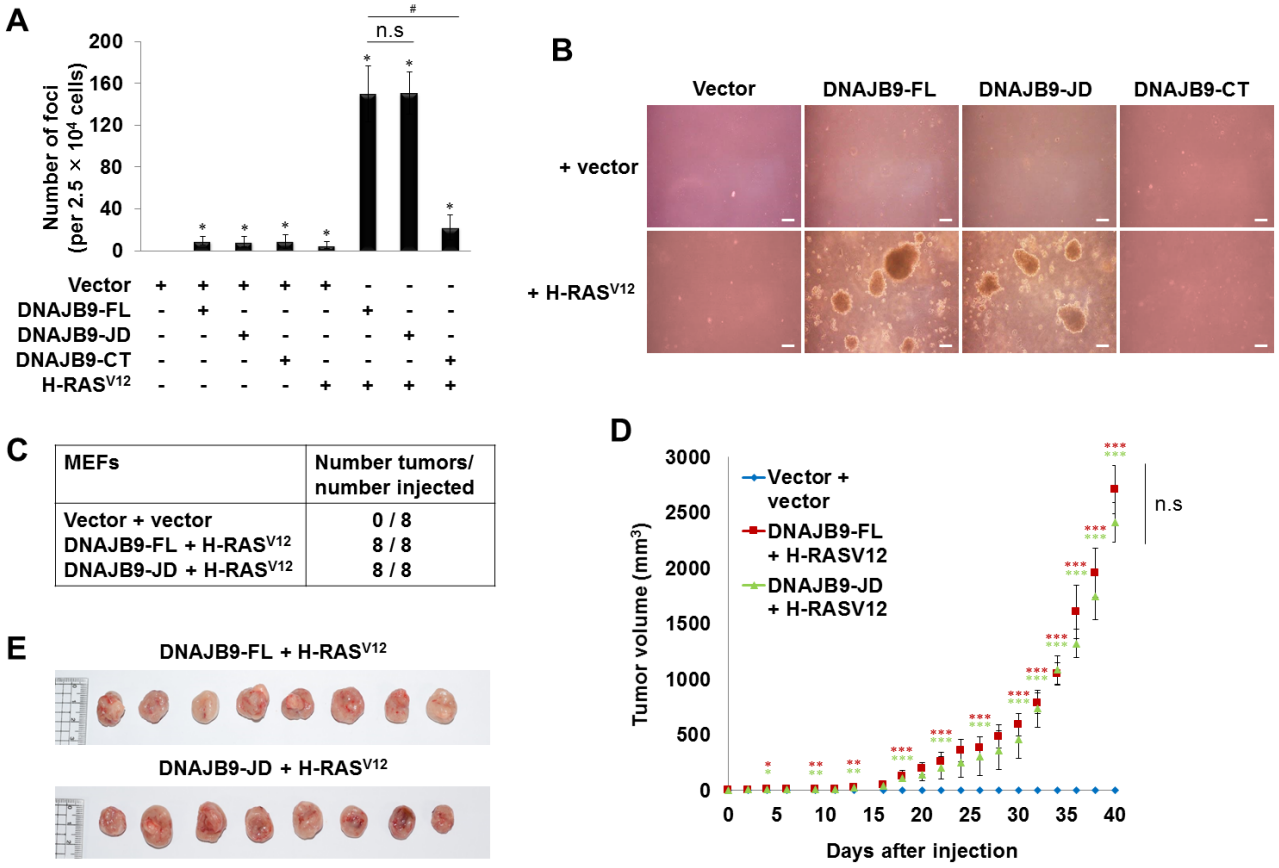

Fig. 6. The DNAJB9-p53 interaction is involved in DNAJB9-mediated neoplastic transformation. (A) Soft agar assay. MEFs were infected with retroviruses as indicated. Cells were seeded on the soft agar and the total number of foci was counted. Data are represent as mean ± SD (n = 4; $*P < 0.05$ vs vector, $^{\#}P < 0.05$; n.s, not significant). (B) Representative data of soft agar assay was shown. Scale bars = 100 μm. (C-E) *In vivo* tumor formation assay. MEFs were infected with retroviruses and injected into nude mice. Total number of tumors per group (C), tumor volumes (D), and resected tumors (E) were shown. Data are represent as mean ± SD (n = 8; $*P < 0.05$, $**P < 0.01$, $***P < 0.001$ vs vector + vector; n.s, not significant).

Cancer studies for past decades have revealed that malignant transformation is the result from activation of oncogenes and inactivation of tumor suppressor genes (Hanahan and Weinberg, 2000; 2011). However, the genes involved in malignant transformation have not been fully identified. We here showed that DNAJB9 induces neoplastic transformation with H-RAS^{V12} in MEFs (Fig. 3), suggesting that DNAJB9 might be a proto-oncogene being involved in human tumorigenesis. To our knowledge, the expression of DNAJB9 in human tumors has not been studied so far. As a preliminary study, therefore, we downloaded the RNA sequencing data from the TCGA website (Cerami et al., 2012; Gao et al., 2013), and analyzed the expression of DNAJB9 in cancer tissues and their normal counterparts for cancers with more than 10 patients. The data showed that expression of DNAJB9 increases in a variety of human cancers with a fold-change ≥ 2.0 and increases in about 10% of the total 620 patients (Supplementary Fig. S1A), supporting our assumption that DNAJB9 may be involved in human tumorigenesis. In addition, intriguingly, the DNAJB9 expression showed a tendency to increase more frequently in cancers with wild-type *TP53* compared to cancers with mutated *TP53* (Supplementary Fig. S1B), supporting our assumption that DNAJB9 may contribute to human tumorigenesis by inhibiting p53 function. Further studies are required to elucidate the involvement of DNAJB9 in human tumorigenesis.

In conclusion, we here identified a novel cellular function of DNAJB9. Under strong mitogenic signals, DNAJB9 inhibits p53-dependent senescence by physical interactions with p53, by which it prevents OIS and contributes to cell transformation. The present study might contribute to our understanding of the cellular function of DNAJB9 and the molecular basis of cell transformation.

Note: Supplementary information is available on the Molecules and Cells website (www.molcells.org).

ACKNOWLEDGMENTS

This research was supported by the National Research Foundation of Korea (NRF) grant funded by the Korea government (MSIT) (No. 2016R1A2B4012817 and No. 2019R1A2C1009396) and by the 2017 Research Grant from

Kangwon National University (No. 520170433).

AUTHOR CONTRIBUTIONS

H.J.L. performed experiments and data analysis. Y.J.J. and S.L. contributed animal experiments. J.I.K. performed RNA sequencing data analysis and statistical analysis. J.A.H. designed the research and wrote the manuscript.

CONFLICT OF INTEREST

The authors have no potential conflicts of interest to disclose.

ORCID

Hyeon Ju Lee https://orcid.org/0000-0003-3252-0898
Yu-Jin Jung https://orcid.org/0000-0002-4942-677X
Seungkoo Lee https://orcid.org/0000-0003-1317-4133
Jong-Il Kim https://orcid.org/0000-0002-7240-3744
Jeong A. Han https://orcid.org/0000-0001-8417-7070

REFERENCES

Ahn, B.Y., Trinh, D.L., Zajchowski, L.D., Lee, B., Elwi, A.N., and Kim, S.W. (2010). Tid1 is a new regulator of p53 mitochondrial translocation and apoptosis in cancer. Oncogene *29*, 1155-1166.

Akagi, T. (2004). Oncogenic transformation of human cells: shortcomings of rodent model systems. Trends Mol. Med. *10*, 542-548.

Awe, K., Lambert, C., and Prange, R. (2008). Mammalian BiP controls posttranslational ER translocation of the hepatitis B virus large envelope protein. FEBS lett. *582*, 3179-3184.

Bartkova, J., Horejsi, Z., Koed, K., Kramer, A., Tort, F., Zieger, K., Guldberg, P., Sehested, M., Nesland, J.M., Lukas, C., et al. (2005). DNA damage response as a candidate anti-cancer barrier in early human tumorigenesis. Nature *434*, 864-870.

Bartkova, J., Rezaei, N., Liontos, M., Karakaidos, P., Kletsas, D., Issaeva, N., Vassiliou, L.V., Kolettas, E., Niforou, K., Zoumpourlis, V.C., et al. (2006). Oncogene-induced senescence is part of the tumorigenesis barrier imposed by DNA damage checkpoints. Nature *444*, 633-637.

Benanti, J.A. and Galloway, D.A. (2004). Normal human fibroblasts are resistant to RAS-induced senescence. Mol. Cell. Biol. *24*, 2842-2852.

Campisi, J. and d'Adda di Fagagna, F. (2007). Cellular senescence: when bad things happen to good cells. Nat. Rev. Mol. Cell Biol. *8*, 729-740.

Cerami, E., Gao, J., Dogrusoz, U., Gross, B.E., Sumer, S.O., Aksoy, B.A., Jacobsen, A., Byrne, C.J., Heuer, M.L., Larsson, E., et al. (2012). The cBio cancer genomics portal: an open platform for exploring multidimensional cancer genomics data. Cancer Discov. *2*, 401-404.

Choi, E.M., Kim, S.R., Lee, E.J., and Han, J.A. (2009). Cyclooxygenase-2 functionally inactivates p53 through a physical interaction with p53. Biochim. Biophys. Acta *1793*, 1354-1365.

Courtois-Cox, S., Jones, S.L., and Cichowski, K. (2008). Many roads lead to oncogene-induced senescence. Oncogene *27*, 2801-2809.

Di Micco, R., Fumagalli, M., Cicalese, A., Piccinin, S., Gasparini, P., Luise, C., Schurra, C., Garre, M., Nuciforo, P.G., Bensimon, A., et al. (2006). Oncogene-induced senescence is a DNA damage response triggered by DNA hyper-replication. Nature *444*, 638-642.

Di Micco, R., Fumagalli, M., and d'Adda di Fagagna, F. (2007). Breaking news: high-speed race ends in arrest--how oncogenes induce senescence. Trends Cell Biol. *17*, 529-536.

Dimri, G.P., Lee, X., Basile, G., Acosta, M., Scott, G., Roskelley, C., Medrano, E.E., Linskens, M., Rubelj, I., Pereira-Smith, O., et al. (1995). A biomarker that identifies senescent human cells in culture and in aging skin in vivo. Proc. Natl. Acad. Sci. U. S. A. *92*, 9363-9367.

Ferbeyre, G., de Stanchina, E., Lin, A.W., Querido, E., McCurrach, M.E., Hannon, G.J., and Lowe, S.W. (2002). Oncogenic ras and p53 cooperate to induce cellular senescence. Mol. Cell. Biol. *22*, 3497-3508.

Gao, J., Aksoy, B.A., Dogrusoz, U., Dresdner, G., Gross, B., Sumer, S.O., Sun, Y., Jacobsen, A., Sinha, R., Larsson, E., et al. (2013). Integrative analysis of complex cancer genomics and clinical profiles using the cBioPortal. Sci. Signal. *6*, pl1.

Halazonetis, T.D., Gorgoulis, V.G., and Bartek, J. (2008). An oncogene-induced DNA damage model for cancer development. Science *319*, 1352-1355.

Hanahan, D. and Weinberg, R.A. (2000). The hallmarks of cancer. Cell *100*, 57-70.

Hanahan, D. and Weinberg, R.A. (2011). Hallmarks of cancer: the next generation. Cell *144*, 646-674.

Hartl, F.U., Bracher, A., and Hayer-Hartl, M. (2011). Molecular chaperones in protein folding and proteostasis. Nature *475*, 324-332.

Jozefczuk, J., Drews, K., and Adjaye, J. (2012). Preparation of mouse embryonic fibroblast cells suitable for culturing human embryonic and induced pluripotent stem cells. J. Vis. Exp. *64*, 3854.

Kang, T.W., Yevsa, T., Woller, N., Hoenicke, L., Wuestefeld, T., Dauch, D., Hohmeyer, A., Gereke, M., Rudalska, R., Potapova, A., et al. (2011). Senescence surveillance of pre-malignant hepatocytes limits liver cancer development. Nature *479*, 547-551.

Kim, S.R., Park, J.H., Lee, M.E., Park, J.S., Park, S.C., and Han, J.A. (2008). Selective COX-2 inhibitors modulate cellular senescence in human dermal fibroblasts in a catalytic activity-independent manner. Mech. Ageing Dev. *129*, 706-713.

Kuk, M.U., Kim, J.W., Lee, Y.S., Cho, K.A., Park, J.T., and Park, S.C. (2019). Alleviation of senescence via ATM inhibition in accelerated aging models. Mol. Cells *42*, 210-217.

Kurisu, J., Honma, A., Miyajima, H., Kondo, S., Okumura, M., and Imaizumi, K. (2003). MDG1/ERdj4, an ER-resident DnaJ family member, suppresses cell death induced by ER stress. Genes Cells *8*, 189-202.

Lee, H.J., Kim, J.M., Kim, K.H., Heo, J.I., Kwak, S.J., and Han, J.A. (2015). Genotoxic stress/p53-induced DNAJB9 inhibits the pro-apoptotic function of p53. Cell Death Differ. *22*, 86-95.

Nardella, C., Clohessy, J.G., Alimonti, A., and Pandolfi, P.P. (2011). Pro-senescence therapy for cancer treatment. Nat. Rev. Cancer *11*, 503-511.

Narita, M., Nunez, S., Heard, E., Narita, M., Lin, A.W., Hearn, S.A., Spector, D.L., Hannon, G.J., and Lowe, S.W. (2003). Rb-mediated heterochromatin formation and silencing of E2F target genes during cellular senescence. Cell *113*, 703-716.

Ory, D.S., Neugeboren, B.A., and Mulligan, R.C. (1996). A stable human-derived packaging cell line for production of high titer retrovirus/vesicular stomatitis virus G pseudotypes. Proc. Natl. Acad. Sci. U. S. A. *93*, 11400-11406.

Qiu, X.B., Shao, Y.M., Miao, S., and Wang, L. (2006). The diversity of the DnaJ/Hsp40 family, the crucial partners for Hsp70 chaperones. Cell. Mol. Life Sci. *63*, 2560-2570.

Sarkisian, C.J., Keister, B.A., Stairs, D.B., Boxer, R.B., Moody, S.E., and Chodosh, L.A. (2007). Dose-dependent oncogene-induced senescence in vivo and its evasion during mammary tumorigenesis. Nat. Cell Biol. *9*, 493-505.

Serrano, M., Lin, A.W., McCurrach, M.E., Beach, D., and Lowe, S.W. (1997). Oncogenic ras provokes premature cell senescence associated with accumulation of p53 and p16INK4a. Cell *88*, 593-602.

Shen, Y., Meunier, L., and Hendershot, L.M. (2002). Identification and characterization of a novel endoplasmic reticulum (ER) DnaJ homologue, which stimulates ATPase activity of BiP in vitro and is induced by ER stress. J. Biol. Chem. *277*, 15947-15956.

Tomayko, M.M. and Reynolds, C.P. (1989). Determination of subcutaneous

tumor size in athymic (nude) mice. Cancer Chemother. Pharmacol. *24*, 148-154.

Trinh, D.L., Elwi, A.N., and Kim, S.W. (2010). Direct interaction between p53 and Tid1 proteins affects p53 mitochondrial localization and apoptosis. Oncotarget *1*, 396-404.

Vos, M.J., Hageman, J., Carra, S., and Kampinga, H.H. (2008). Structural and functional diversities between members of the human HSPB, HSPH, HSPA, and DNAJ chaperone families. Biochemistry *47*, 7001-7011.

Walsh, P., Bursac, D., Law, Y.C., Cyr, D., and Lithgow, T. (2004). The J-protein family: modulating protein assembly, disassembly and translocation. EMBO Rep. *5*, 567-571.

Zhao, J.J., Roberts, T.M., and Hahn, W.C. (2004). Functional genetics and experimental models of human cancer. Trends Mol. Med. *10*, 344-350.